IoT-Enabled Sensor Node for Environmental Monitoring

Parag Chourey, Nirbhow Jap Singh, Kirti Soni, and Ravinder Agarwal

Abstract In the environmental monitoring system, the atmospheric boundary layer (ABL) plays an important role. It is a major source of concern for the scientific community, and it necessitates the implementation of an effective and quick monitoring system to make better decisions. SODAR is a critical tool for continuous determining the environmental parameters in real time. The ABL height is a critical parameter for determining the air quality in a given area. The use of the well-connected SODAR network to determine ABL height from remote locations in real time is beneficial for analyzing and planning the environmental monitoring system. The Internet of Things (IoT) is a ground-breaking technology, which allows various environmental monitoring stations to communicate with one another. The interconnection of several IoT-enabled sensor nodes is known as an IoT network. Multiple sensors, a data acquisition system, and a data communication system make up the sensor node. It accomplishes the goal of monitoring local environmental parameters and sharing information with an IoT network. A sensor node is composed of a SODAR, a wind sensor, a temperature, and a relative humidity sensor. The indigenous SODAR design, integrated into common data acquisition software, with other meteorological sensors was used. For the reliable performance of the proposed system, the calibration of meteorological sensors was important. Before installation, all meteorological sensors used were calibrated. In addition, the data from the sensor node-enabled by IoT were also validated with comparisons to the local data acquisition system.

Keywords Internet of Things · Meteorological sensors · Mixing height · Planetary boundary layer features · Meteorological sensors · Sensor node

P. Chourey (✉) · N. J. Singh · R. Agarwal
TIET, Patiala, Punjab, India
e-mail: choureyparag@gmail.com

K. Soni
CSIR-NPL, Delhi, India

S. Yadav et al. (eds.), *Recent Advances in Metrology*, Lecture Notes in Electrical Engineering 906, https://doi.org/10.1007/978-981-19-2468-2_38

1 Introduction

Environmental monitoring is important in various aspects of life including the monitoring and control of air pollution, meteorological forecasts, water quality control, and monitoring. Environmental monitoring aims to facilitate the appropriate application under favorable environmental conditions. Advanced technologies such as IoT and sensor networking play a critical role in sustainable growth and a healthy society. The monitoring and meteorological parameters on the atmospheric borders (ABL) provide conceptual knowledge about the critical parameters affecting the air quality in an area [11, 19]. The ABL lies within the 1–2 km of the lower atmosphere where all living entities exist. ABL monitoring has a key role in estimating pollutant emissions from the atmosphere. Collective information on weather and ABL height helps to determine the atmospheric dispersion and the air particles' emission process. This process shows the carrying capacity to the atmosphere of air pollutants [13]. So, it becomes essential to monitor the ABL structure collectively and some important weather parameters effectively in environmental monitoring.

The ABL monitoring techniques are broadly classified into two categories, i.e., direct or in situ measurements and remote sensing techniques. The remote sensing techniques have significant advantages over in situ techniques due to their wide monitoring range and cost-effectiveness. The SODAR is one of the best tools for continuous monitoring of the ABL structure in real time [1] and recommended by the regulation authorities like Environmental Impact Association (EIA) USA and Central Pollution Control Board (New Delhi) India for ABL structure monitoring [6].

In the decade, the Internet of Things (IoT) has been evolved as a technology. With real-time data accessibility, cloud storage, and the ability to make autonomous decisions, it revolutionized the way objects interact with one another [7, 12, 17]. In this chapter, the parameters such as temperature, relative humidity, wind speed, and wind directions are addressed with the ABL structure for the collective measurement of important air pollution meteorological parameters. The networking between the sensors is required for the collective measurement and monitoring of these parameters on a single platform. The proposed method integrates SODAR in the design of a sensor network with meteorological sensors like wind sensors, temperature sensors, and relative humidity sensors. A modern signal processing unit, data acquisition unit, data networks, and data storage facilities are also provided in the sensors network for the creation of an IoT-enabled sensor node. Figure 1 shows the block diagram of the proposed IoT capable node.

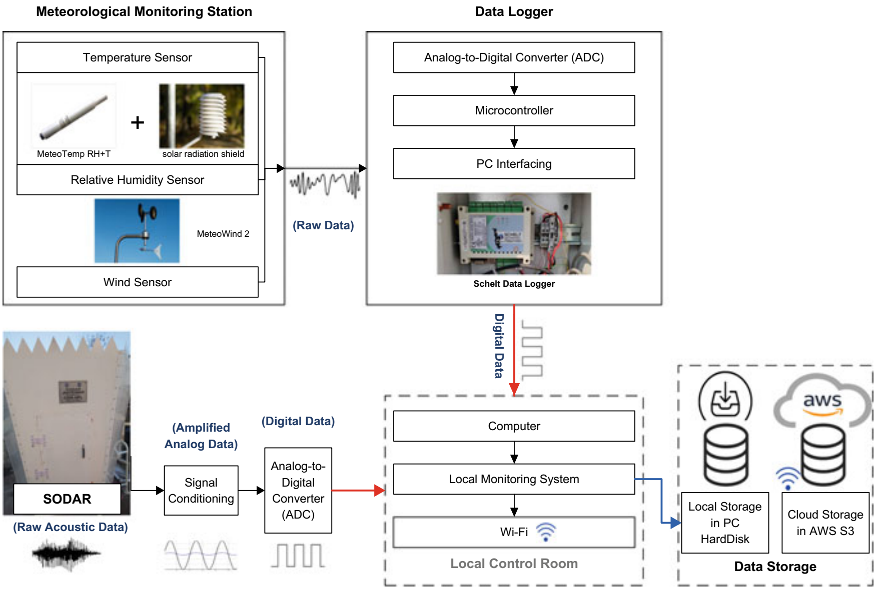

Fig. 1 Block diagram of IoT-enabled sensor node consisting of SODAR and meteorological sensors (temperature, relative humidity, and wind)

2 System Design

The IoT-enabled sensor node consists of sensors, data gathering systems, data tracking and communication, and storage facilities. The following are the main components of the proposed IoT-enabled sensor-node system.

(a) Meteorological Sensors
   i. MeteoTemp (RH + T) for temperature and relative humidity measurements
   ii. MeteoWind2 for wind speed and wind direction measurement
   iii. Data logger for meteorological sensors
(b) Signal processing unit (SPU) for monostatic SODAR for ABL height measurement
(c) Common data acquisition software
(d) Data storage and data communication software.

Meteorological Sensors: The MeteoTemp (RH+T) and MeteoWind2 sensors manufactured by Barani design technologies, Slovakia was used. An anemometer with a wind vane had the excellent accuracy of World Meteorology Organization (WMO) and MEASNET standards (MEASNET/IEC 61400-12-1:2005 calibrations and ISO/IEC 17025:2005 calibrations) for meteorology and wind resource assessment [18]. It had a very low power consumption and integrated lightning and surge protection for reliable operation. Temperature and humidity sensor consumes ultra-low power with accurate measurement of air temperature and humidity as per the standard of WMO (ISO/IEC 17025:2005) for long-term stability [10]. These meteorological sensors can provide reliable continuous monitoring in adverse environmental conditions [3].

Schelt Technology, India, has developed the data logger for meteorological sensors. It supplies the fundamental analog-to-digital converters, microcontrollers, and interfaces for PC processing transmits and communicates with the local monitoring station for the raw analog signal received from sensors. The program was designed to process additional digital signal data for use with the hardware board for monitoring purposes. The block diagram of the meteorological sensor data acquisition system is shown in Figure 2.

Monostatic SODAR: Monostatic SODAR was used as a sensor for creating the sensor node. The purpose of installing SODAR was to measure the ABL height in real time. This SODAR was designed and developed indigenously in the CSIR-National Physical Laboratory (CSIR-NPL), New Delhi India. Monostatic SODAR works on the acoustic principle where the high acoustic signal was transmitted into the atmosphere, and a backscattered signal was received from the atmosphere due to temperature turbulence [6]. The received signal was further processed through the signal conditioning stage. The signal conditioning stage consists of a preamplifier and a narrow band-pass filter. Figure 3 depicts the gain and noise characteristics of an indigenous preamplifier design. The single low-noise amplifier with state-variable (SV) narrow band-pass filter configuration was used in the pre-amplification stage.

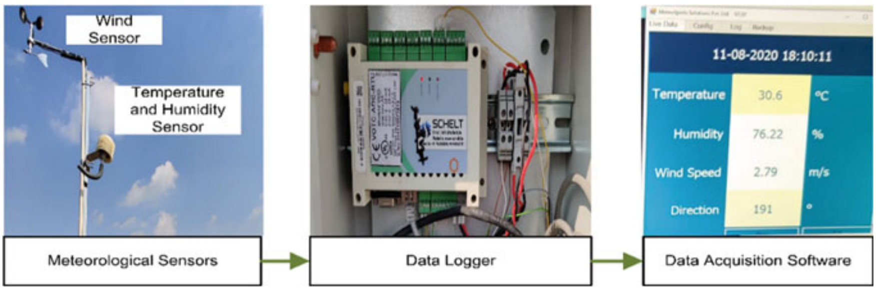

Fig. 2 Block diagram of meteorological sensor data acquisition system

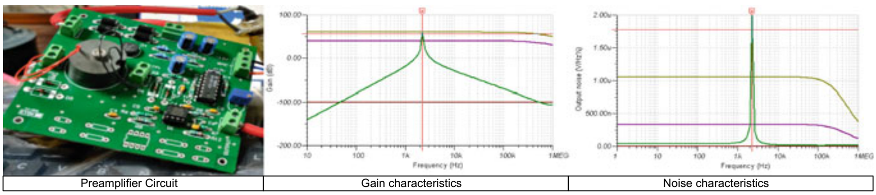

Fig. 3 SODAR preamplifier gain and noise characteristics

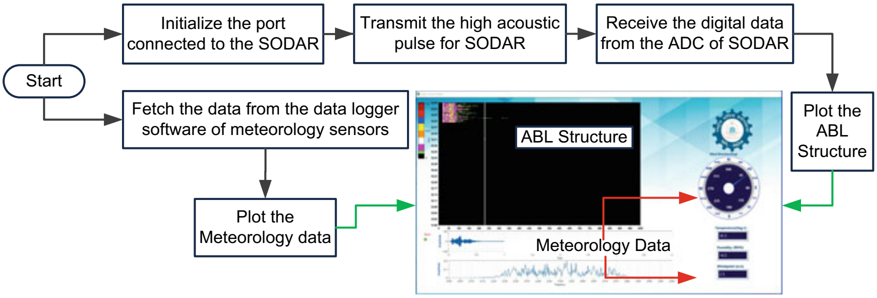

Fig. 4 Flowchart of the common data acquisition software

The total gain and output noise of the design were 54 dB and $2\mu V/\sqrt{Hz}$. Further, the processed analog signal was converted into the digital signal using the built-in sound card of the computer [4].

Common Data Acquisition Software: The digital signal from the sensors was sent to the local monitoring station. The common data acquisition software provides further data processing and manipulation for local data visualization in a desirable format. This software also controls the transmission and receiving of the acoustic signal for SODAR. Figure 4 shows the software's flowchart. This software helps meteorology and SODAR information to be combined in real time with visualization.

Data Storage and data communication Software: The local monitoring station has a data storage facility for offline monitoring of historical data. This system also includes Wi-Fi for Internet access. Each local monitoring station worked as a gateway for the IoT networking and shares the real-time data with the AWS-S3 cloud storage system in near real time. The data communication from the monitoring station to the cloud was established using the NI-LabVIEW-based software. Figure 5 depicts the flowchart of the AWS-S3 data communication software. The new bucket of each day was created automatically from the software. The data were updated using the put-object function of AWS-S3 after every 20 s. The identity and access management function provides secure data access as well as privacy, consent, and identity verification while data communication [2, 5]. Further, the data were stored in the AWS-S3 cloud storage. The sensors, signal conditioning unit, data acquisition system, and data communication system work together to create an IoT-enabled sensor node to visualize and share data on its own.

3 Results and Discussion

The results of the planned IoT-enabled sensor-node system are discussed. In the first part, the data analysis of SODAR and meteorological sensors, i.e., ABL height, temperature, relative humidity, wind speed, and direction, is described. In the second

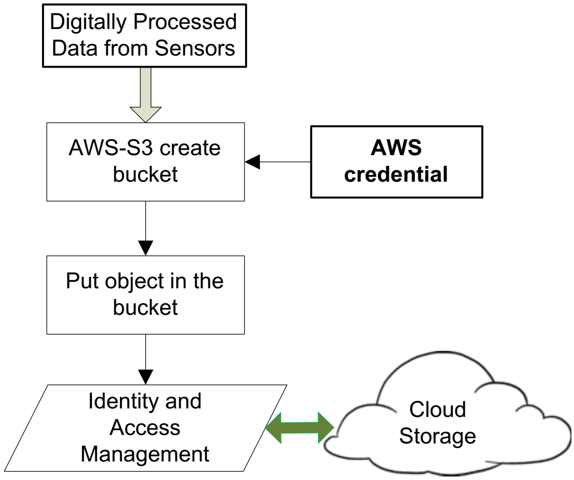

Fig. 5 Flowchart of the LabVIEW and AWS-S3-based data communication software

part of the analysis, the statistical analysis has been done on the IoT-enabled sensor-node data and uncertainty and measurement accuracy.

Data Analysis: The detailed study of ABL structures and corresponding meteorological data is presented in Fig. 6. The data have been plotted using the LabVIEW-based offline software. This software provides a single platform for simultaneously visualizing all sensor data. The data from 19th October 2020 have been selected for the demonstration purpose. Figure 6a presents the 24-h data analysis of ABL structure, wind direction, hourly mean wind speed, hourly mean relative humidity, and hourly mean temperature data. This software also cumulates the ABL height information after manual calculation. The graph shows that wind speed and temperature have a proportional relationship, whereas relative humidity has an inverse relationship with temperature and wind speed. The variation in ABL structure is also visible in the graph.

Figure 6b–d presents the special structures found during the different time frames on 19th October 2020. Figure 6b depicts the thermal plumes with periodical spikes during daytime. These structures show a more common phenomenon of atmosphere and formed due to rise in the temperature at daytime. The higher-thermal plumes were considered favorable for higher pollutant dispersion [8, 9, 15]. In this period, the temperature and wind speed shows an increasing trend, whereas the relative humidity decreases with time. Figure 6c demonstrates the rising layer structure of ABL. The rising layer structure was formed during the transition period of day (from early morning to afternoon period). The transition period may vary from season to season. In this graph, it was observed that the ABL height starts increasing and split from the bottom structure of ABL in the morning time [14]. With the start of the rising layer, the temperature, wind speed graph was increasing, and the opposite trend was visible with relative humidity. Figure 6d presents the inversion period of the day. It is visible from the graph that during the inversion time, a stable ABL structure

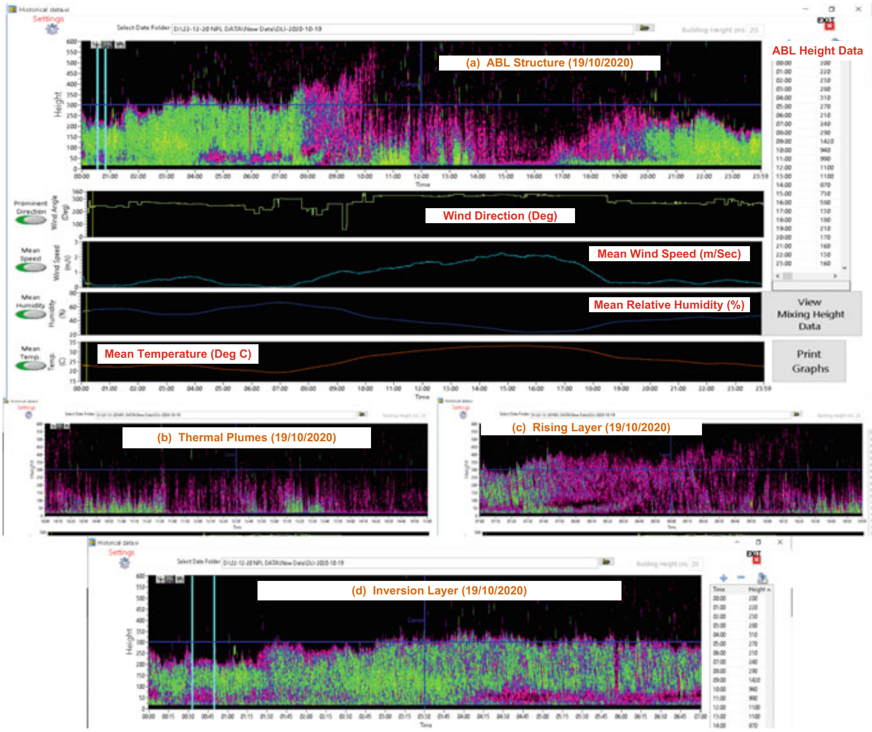

Fig. 6 Various ABL structures of 19th October 2020 and corresponding meteorological data, **a** 24-h ABL structure **b** thermal plumes structure, **c** rising layer structure, **d** inversion layer structure

is formed [16]. In this period, most of the meteorological parameters were settled down, and less variation was visible in comparison to the thermal plumes period.

Statistical Analysis of IoT-Enabled Data Communication System: The accuracy of the IoT-enabled sensor node was verified. In this, the data communication accuracy was checked by comparing the received data points with transmitted data points. The one-month data of the proposed sensor node were collected from the local monitoring station and cloud. The communication error was classified into two categories, i.e., system error and communication error. The sluggish network, malfunction in software, routine maintenance, and power interrupts were the major cause of the system error. Whereas, the error due to the data transmission system was considered as a communication error. The data communication percentage accuracy and percentage error are calculated using following equations.

$$\%\text{Accuracy} = \frac{\text{Total Received Data Points(Rx)}}{\text{Total Transmitted Data Points(Tx)}} \times 100 \tag{1}$$

$$\%\text{Error} = \frac{\text{Tx} - \text{Rx}}{\text{Tx}} \times 100 \tag{2}$$

Table 1 Percentage accuracy of proposed IoT-enabled sensor node

Uncertainty estimation of IoT-enabled sensor-node system	Data from (Oct 01, 2020–Oct 30, 2020)				
	Accuracy (%)	Error (%)	σ (%)	u (%)	u_c (%)
SODAR (ABL structure)	99.999	0.00005	0.00104	0.00019	1.06766
Wind speed (WS)	99.994	0.00542	2.14246	0.39784	
Wind direction (WD)	99.964	0.03569	1.79420	0.33317	
Relative humidity(RH)	99.976	0.02344	4.74598	0.88130	
Temperature (T)	99.964	0.03590	1.65038	0.30646	

The standard deviation (σ), standard uncertainty, and combined uncertainty are expressed in Eqs. 3, 4, and 5.

$$(\sigma) = \sqrt{\frac{(x_i - \mu)^2}{N}} \tag{3}$$

where x_i is %accuracy of one day, μ is mea of %accuracy, and N is the total numbr of days.

$$\text{Standard Uncertainty}(u) = \frac{\sigma}{\sqrt{N}} \tag{4}$$

$$\text{Combined Uncertainty}(u_c) = \sqrt{u_{\text{ABL}}^2 + u_{\text{WS}}^2 + u_{\text{WD}}^2 + u_{\text{RH}}^2 + u_T^2} \tag{5}$$

Table 1 shows the proposed system's estimated uncertainty results. The statistical analysis of the IoT-enabled sensor node reveals that the accuracy was greater than 99.9 % for all sensor data, with an error of less than 0.1 %. The sensor-node system's standard deviation and standard uncertainty were also evaluated. All sensors showed less variation and uncertainty, according to the data. The ABL data have the lowest standard uncertainty. The suggested sensor-node system was a combined uncertainty of 1.067 %. Overall, the statistical analysis indicates that the IoT-enabled sensor-node system was considerably high accuracy and extremely little uncertainty.

4 Conclusion

This chapter describes a sensor node enabled for the monitoring of the environment by SODAR and meteorological sensors. The sensor node with IoT measures and shares with the cloud in almost reality the ABL height, wind speed, wind direction, relative temperature, and humidity data. The suggested sensor-node data collection program concurrently monitors all parameters on a single platform. Data transmission was a difficult challenge because of the enormous amount of data. The described data transmission system achieves 99.99% accuracy with a total error rate of less than 0.1%. Research on the uncertain estimation shows that the total uncertainty of the system is around 1%. The suggested IoT-enabled sensor node is extremely useful for the scientific community working in atmospheric research since it allows them to remotely monitor critical environmental parameters in real time. This sensor node may be placed at numerous places in the future to create an IoT-based environment monitoring system. In the future, this sensor node can be installed at multiple locations for creating an IoT-based environment monitoring network.

Acknowledgment This research was carried out at the CSIR-NPL. The authors are grateful to the Director of the CSIR National Physical Laboratory (NPL).

References

1. Asimakopoulos DN, Helmis CG, Michopoulos J (2004) Evaluation of SODAR methods for the determination of the atmospheric boundary layer mixing height. Meteorol Atmos Phys 85:85–92
2. Brantner M, Florescu D, Graf D, Kossmann D, Kraska T (2008) Building a database on S3. In: Proceedings of the 2008 ACM SIGMOD international conference on Management of data. Pp 251–264
3. Chourey P, Singh NJ, Soni K, Agarwal R (2022) SODAR based meteorological sensor network for air pollution monitoring in Northern India. MAPAN 1–15
4. Chourey P, Soni K, Singh NJ, Agarwal R (2022) IoT-Sodar network for airshed management planning. IETE J Res 1–15
5. Garfinkel S (2007) An evaluation of Amazon's grid computing services: EC2, S3, and SQS. Harvard Comput Sci Gr Tech Rep TR-08–07
6. Gera BS, Raghavendra T, Singh G, Ojha VK, Malik J, Gera N, Gupta NC (2011) Instrumentation and computer capabilities for improving sodar data acquisition. Int J Remote Sens 32:4807–4817
7. Khan MA, Salah K (2018) IoT security: review, blockchain solutions, and open challenges. Futur Gener Comput Syst 82:395–411
8. Kumar N, Soni K, Agarwal R (2021) Prediction of temporal atmospheric boundary layer height using long short-term memory network. Tellus A Dyn Meteorol Oceanogr 73:1–14
9. Kumar N, Soni K, Garg N, Agarwal R, Saha D, Singh G (2017) SODAR pattern classification and its dependence on meteorological parameters over a semiarid region of India. Int J Remote Sens 1161:3466–3482
10. Leštinská L, Danc IJ (2016) Temperature and humidity calibration procedure ISO/IEC 17025:2005
11. Li Z, Guo J, Ding A, Liao H, Liu J, Sun Y, Wang T, Xue H, Zhang H, Zhu B (2017) Aerosol and boundary-layer interactions and impact on air quality. Natl Sci Rev 4:810–833
12. Madakam S, Lake V, Lake V, Lake V et al (2015) Internet of things (IoT): a literature review. J Comput Commun 3:164
13. Pleim JE (2007) A combined local and nonlocal closure model for the atmospheric boundary layer. Part II: application and evaluation in a mesoscale meteorological model. J Appl Meteorol Climatol 46:1396–1409
14. Singal SP, Lewthwaite EWD, DSW (1989) Estimating atmospheric stability from monostatic acoustic sounder records. Atmos Environ 23:2079–2084
15. Singal SP, Aggarwal SK, Pahwa DR, SG B (1984) Stability studies with the help of acoustic sounding. Atmos Environ 19:221–228

16. Singal SP, Gera BS, Kallistratova MA, Petenko IV (1997) Sodar aspect sensitivity studies in the convective boundary layer. Int J Remote Sens 18:1809–1819
17. Talavera JM, Tobón LE, Gómez JA, Culman MA, Aranda JM, Parra DT, Quiroz LA, Hoyos A, Garreta LE (2017) Review of IoT applications in agro-industrial and environmental fields. Comput Electron Agric 142:283–297
18. Westermann D, Westermann H (2018) Measnet anemometer calibration procedure ISO/IEC 17025:2005
19. Zhou W, Jia Y, Peng A, Zhang Y, Liu P (2018) The Effect of IoT new features on security and privacy: new threats, existing solutions, and challenges yet to be solved. IEEE Internet Things J 4662:1–11